jas

CONF-8709107--1

DE87 011404

MOTION-DEPENDENT FLUID FORCES ACTING ON A TUBE ROW IN CROSSFLOW*

by

J. A. Jendrzejczyk and S. S. Chen

Materials and Components Technology Division
ARGONNE NATIONAL LABORATORY
Argonne, Illinois 60439

January 1987

Paper to be presented at the ASME Vibration Conference, Boston, Massachusetts, September 27-30, 1987.

*This work was performed under the sponsorship of NASA-Lewis Research Center.

MOTION-DEPENDENT FLUID FORCES ACTING ON A TUBE ROW IN CROSSFLOW

by

J. A. Jendrzejczyk and S. S. Chen

Materials and Components Technology Division
Argonne National Laboratory
9700 South Cass Avenue
Argonne, Illinois 60439

ABSTRACT

Motion-dependent fluid forces acting on a tube row with a pitch-to-diameter ratio of 1.35 are measured for several flow velocities and a series of oscillation frequencies. Fluid-damping and fluid-stiffness coefficients are obtained from motion-dependent fluid forces as a function of reduced flow velocity. Fluid-force coefficients agree reasonably with published data. Based on the fluid-force coefficients, the critical flow velocity and instability characteristics of tube arrays in crossflow can be predicted.

I. INTRODUCTION

When a cylinder or a group of cylinders is submerged in crossflow, the cylinders are subjected to different fluid forces. These fluid force components can conveniently be divided into two groups:

Fluid Excitation Forces: When a cylinder is stationary in flow, it disturbs the flow field resulting in fluid pressure and shear stress acting on the surface of the cylinder. The resultant effect of the fluid pressure and shear stress is called fluid excitation force. For example, steady drag or fluctuating lift acting on an isolated cylinder are typical fluid excitation forces.

Motion-Dependent Fluid Forces: If the cylinders are moving, in addition to the fluid excitation forces, additional fluid forces are introduced; these fluid forces depend on cylinder displacement, velocity, and acceleration and they are called motion-dependent fluid forces.

The effects of fluid excitation forces and motion-dependent fluid forces are different. The former is one type of forcing function while the latter affects the system mass, damping, and stiffness. The objective of this study is to present the motion-dependent fluid forces acting on a tube row.

Tests to measure motion-dependent fluid forces have been reported for an isolated cylinder [1-5], twin cylinders [6] and a group of cylinders [7,8]. In these tests, a cylinder is given a prescribed motion and then the fluid forces acting on the cylinder itself and the surrounding cylinders are measured. Motion-dependent fluid forces are found to depend on Reynolds number, oscillation amplitude, oscillation frequency, flow velocity and

incoming flow property. Results from the measured data are used to predict structural response in flow.

In this study, fluid forces are measured for a tube row with a pitch-to-diameter ratio of 1.35. Fluid-damping and fluid-stiffness coefficients are reduced from fluid-force data as a function of the reduced flow velocity. These fluid-force coefficients are useful in predicting fluidelastic instability.

II. MOTION-DEPENDENT FLUID FORCES

Consider a group of n tubes vibrating in a flow as shown in Fig. 1. The axes of the tubes are parallel to one another and perpendicular to the x-y plane. Each tube has the same radius R, and the fluid is flowing with a gap flow velocity U. The displacement components of tube j in the x and y directions are u_j and v_j, respectively. The motion-dependent fluid-force components acting on tube j in the x and y directions are f_j and g_j, respectively; f_j and g_j are given as [9]

$$f_j = -\rho\pi R^2 \sum_{k=1}^{n} \left(\alpha_{jk} \frac{\partial^2 u_k}{\partial t^2} + \sigma_{jk} \frac{\partial^2 v_k}{\partial t^2}\right)$$

$$+ \frac{\rho U^2}{\omega} \sum_{j=1}^{n} \left(\alpha'_{jk} \frac{\partial u_j}{\partial t} + \sigma'_{jk} \frac{\partial v_k}{\partial t}\right)$$

$$+ \rho U^2 \sum_{k=1}^{n} \left(\alpha''_{jk} u_k + \sigma''_{jk} v_k\right) , \qquad (1)$$

and

$$g_j = -\rho\pi R^2 \sum_{k=1}^{n} \left(\tau_{jk} \frac{\partial^2 u_k}{\partial t^2} + \beta_{jk} \frac{\partial^2 v_k}{\partial t^2}\right)$$

$$+ \frac{\rho U^2}{\omega} \sum_{k=1}^{n} \left(\tau'_{jk} \frac{\partial u_j}{\partial t} + \beta'_{jk} \frac{\partial v_k}{\partial t}\right)$$

$$+ \rho U^2 \sum_{k=1}^{n} \left(\tau''_{jk} u_k + \beta''_{jk} v_k\right) , \qquad (2)$$

where ρ is fluid density, t is time, and ω is circular frequency of tube oscillations. α_{jk}, β_{jk}, σ_{jk} and τ_{jk} are added mass coefficients, α'_{jk}, β'_{jk}, σ'_{jk} and τ'_{jk} are fluid-damping coefficients, and α''_{jk}, β''_{jk}, σ''_{jk} and τ''_{jk} are fluid-stiffness coefficients.

Three flow theories have been used for fluid-force coefficients: quasi-static flow theory, quasi-steady flow theory, and unsteady flow theory. The characteristics of the fluid-force coefficients based on these theories have been discussed previously [10]. In this study, the unsteady flow theory is used.

Fluid-force coefficients can be determined by measuring the fluid forces acting on the tubes due to oscillations of a particular tube. For example, tube k is excited in the y direction; its displacement in the y direction is given by

$$v_k = v \cos \omega t . \qquad (3)$$

The fluid force acting on tube j in the x direction can be written

$$f_j = \frac{1}{2} \rho U^2 c_{jk} \cos(\omega t + \phi_{jk}) , \qquad (4)$$

where c_{jk} is the fluid-force amplitude and ϕ_{jk} is the phase angle that the fluid force acting on tube j leads the displacement of tube k.

Using Eqs. 1 and 3, we can also write the fluid force component as

$$f_j = (\rho\pi R^2\omega^2\sigma_{jk} + \rho U^2\sigma''_{jk})v \cos \omega t - \rho U^2\sigma'_{jk} v \sin \omega t \ . \tag{5}$$

Comparing Eqs. 4 and 5 yields

$$\sigma''_{jk} = \frac{1}{2} c_{jk} \cos \phi_{jk} - \frac{\pi^3}{U_r^2} \sigma_{jk} \ , \tag{6}$$

and

$$\sigma'_{jk} = \frac{1}{2} c_{jk} \sin \phi_{jk} \ , \tag{7}$$

where U_r is the reduced flow velocity ($U_r = \pi U/\omega R$).

The added mass coefficient α_{jk} in Eq. 6 can be calculated using the potential flow theory [11]. Then σ'_{jk} and σ''_{jk} can be calculated from Eqs. 6 and 7 when the force amplitude c_{jk} and phase angle ϕ_{jk} are measured. Other fluid-force coefficients can be obtained in the same manner.

Fluid force coefficients depend on tube arrangement, tube pitch, oscillation amplitude, oscillation frequency, and flow velocity. For a given tube array, fluid force coefficients are functions of oscillation amplitude (A/D) and reduced flow velocity (U_r). For small-amplitude oscillations, fluid-force coefficients can be considered a function of the reduced flow velocity only.

III. EXPERIMENTAL SETUP

The tests were performed in a water channel. Water is pumped into an input tank through a flow control valve and turbine flowmeter. The flow passes through a series of screens and honeycombs and then into a rectangular flow channel. The water level is controlled by standpipes in the output tank.

Mass flowrate is measured by a turbine flowmeter. The velocity profile in the test area is measured with a turboprobe flowmeter.

A row of tubes (see Fig. 1) is assembled in the test area. Tubes 1, 2, and 3 are active tubes while the others are dummy tubes. The relatively rigid main bodies of the tubes are constructed from stainless steel tubing with a 2.54 cm (1 in.) OD, a 0.071 cm (0.028 in.) wall thickness and a 38.1 cm (15 in.) length (see Fig. 2). Thin brass end caps are soldered to both ends of each tube and a smaller, relatively flexible tube, with a 0.635 cm (0.25 in.) OD, a 0.089 cm (0.035 in.) wall thickness, and a 12.07 cm (4.75 in.) length, is fastened to the upper end cap of each tube. All tubes except tube 1 are clamped to a support plate with a nut attached to the smaller supporting tube. Tube 1 is not attached to the support plate, but passes through a circular hole in the support plate and is connected to an electromagnetic shaker. The shaker provides the support for tube 1. In addition, prescribed oscillations can be given to tube 1 in the x or y direction. Both the oscillation amplitude and frequency of the shaker can be controlled in the appropriate range.

For the active tubes, two sets of strain gauges are placed on the outer surface of the smaller tube where the outer surface of the tube has been machined to a smaller diameter. The two sets of strain gauges measure the force components in the two perpendicular directions with a sensitivity of approximately 1 volt for 0.18 Newtons (0.04 lb) of force acting on the middle of the active tubes.

The dummy tubes are constructed of the same material as the active tubes. However, the supporting element attached to the dummy tube is not machined to reduce its stiffness. Therefore, the dummy tubes are more rigid compared with the active tubes.

During tests, the water surface is kept at a level so that the active length of the tubes is submerged in the flow. Normally, only a small portion

of the supporting tube (less than 1.3 cm) is submerged in water. Therefore the strain gauges do not require waterproofing.

IV. TEST PROCEDURES AND DATA ANALYSIS

The force transducers (active tubes) are calibrated by two methods--static and dynamic.

- Static Method in Air: The active tube is held fixed at the supported end and a given force is applied at the middle of the active length.
- Dynamic Method in Air and in Water: The tube is excited at a given frequency and amplitude in air or in water. Then the inertia force due to the sinusoidal oscillations are used to determine the calibration constant.

In general, fairly consistent results are obtained. In application, the calibration constant from the dynamic method is used.

Motion-dependent fluid forces are measured for tubes 1, 2, and 3, with tube 1 oscillating in the lift or drag direction. In all tests, the excitation frequency varies from 0.1 to 1.95 Hz. The gap flow velocities are set at 5.11, 10.03, and 15.37 cm/sec. The oscillation amplitude of tube 1 is set approximately at 0.02 D to 0.05 D.

Tests are also performed to understand the effects of several parameters and the characteristics of fluid-force coefficients.

- Oscillation amplitude: Tube 1 is excited at different oscillation amplitudes; this is to investigate the effect of oscillation amplitudes on fluid-force coefficients.
- Misalignment: Tube 1 is offset a small amount so that the role of misalignment can be understood.

A flow diagram of the instrumentation and exciter is shown in Fig. 3. The DC power supply controls the static displacement, or the position of the middle active tube with respect to the adjacent two active tubes. The signal generator provides the sinusoidal displacement at a frequency varying from about 0.1 Hz to 2.0 Hz. Displacement and force signals are filtered by matching low-pass filters to eliminate high-frequency noises above 3 Hz and

then are digitized and stored in the FFT analyzer. These signals are analyzed to obtain the oscillation displacement of the tube, the magnitudes of the forces acting on the active tubes, and the phase between the motion-dependent fluid force and tube displacement. In general, 30 to 50 cycles are averaged to obtain a stable and repeatable output.

V. TEST RESULTS

The natural frequency of the active tubes is about 8.8 Hz in air and 6.6 in water. The excitation frequency in different tests varies from 0.1 to 1.95 Hz; the maximum amplification factor of the active tubes at high frequency (1.95 Hz) is about 110%. In the data analysis, the effect of dynamic amplification is not accounted.

Vortex Shedding

From the frequency spectra of the fluid excitation forces, the vortex shedding frequency can be identified and the Strouhal number can be calculated:

$$St = \frac{fD}{U} , \tag{8}$$

where $f = \omega/2\pi$ and $D = 2R$. Two Strouhal numbers are found: 0.16 and 0.49.

Various investigators have found different vortex shedding frequencies for tube rows in crossflow [12-16]. Published data and present results are given in Fig. 4 as a function of the pitch-to-diameter ratio (T/D). The lower value of St at 0.16 compares well with other data, while 0.49 is higher than the published data.

The Strouhal number obtained in this study is associated with the fluid forces acting on the tube, and is not determined from the flow field in the wake. The fluid force represents the resultant effect of fluid pressure and shear stress acting on the surface of the cylinder; therefore, some of the vortex shedding frequencies measured in the wake do not appear in the force.

Motion-Dependent Fluid Forces

Figure 5 shows the fluid force components f_j and g_j (j = 1, 2, 3) acting on tubes 1, 2, and 3 because of the motion of tube 1 in the lift direction for several values of U_r. Note that in Fig. 5, tube inertia force is included in f_1. The dominant frequency of the fluid forces is the same as the tube oscillation frequency; however, the fluid forces are not in phase with tube displacement.

As shown in Eq. 4, the phase angle is defined as the angle between the fluid force component and tube displacement. This angle can be obtained from the correlation between the two time histories of fluid force and tube displacement. Figure 6 shows typical fluid forces and phase angles as a function of reduced flow velocity; f_1 includes tube inertia force. When the reduced flow is small, the fluid force decreases rapidly with increasing reduced flow velocity. This is attributed to the effect of the inertia force. At higher reduced flow velocity, the magnitude of the fluid force is almost independent of U_r. Similar trends are noted for the phase angle. At low U_r, the phase angle varies more drastically with U_r, while at large U_r, the variation of the phase angle with U_r is much smaller.

Fluid-Force Coefficients

From the fluid forces and their phase angles as well as the added mass coefficients based on the potential flow theory, fluid-damping and fluid-stiffness coefficients can be calculated using the techniques described in Section II. Note that the structural inertia force of tube 1 is properly substrated in the analysis. Figures 7 and 8 summarize the results.

Fluid-force coefficients obtained in this study agree reasonably well with those based on Tanaka's data [9,17]. However, some of the details are not in complete agreement. The reason for the difference is not known at this time.

Several characteristics of the fluid-force coefficients should be noted:

- Fluid-force coefficients obtained at different flow velocities are about the same. Therefore, for relatively small-amplitude oscillations, fluid-force coefficients are a function of U_r only.
- At high values of U_r (e.g., $U_r > 20$), all fluid-force coefficients are approximately constant. In this range, fluid-force coefficients obtained at a particular U_r are applicable for all values of U_r.

• At small values of U_r (e.g., $U_r < 10$), all fluid-force coefficients are functions of U_r. In this range, fluid-force coefficients have to be determined for all values of U_r.

Symmetry and Antisymmetry of Fluid-Force Coefficients

The symmetric property of the added mass has been proved using the potential flow theory [11]. The added mass matrix for the three active tubes (1, 2, and 3) is given by

$$\begin{bmatrix} \alpha_{jk} & \sigma_{jk} \\ \tau_{jk} & \beta_{jk} \end{bmatrix} = \begin{bmatrix} 1.11 & -0.28 & -0.28 & 0 & 0 & 0 \\ -0.28 & 1.11 & -0.04 & 0 & 0 & 0 \\ -0.28 & -0.04 & 1.11 & 0 & 0 & 0 \\ 0 & 0 & 0 & 1.13 & 0.34 & 0.34 \\ 0 & 0 & 0 & 0.34 & 1.13 & 0.13 \\ 0 & 0 & 0 & 0.34 & 0.13 & 1.13 \end{bmatrix} \qquad (9)$$

$j,k = 1, 2, 3$

It is apparent that the added mass matrix is symmetric.

For fluid-damping and fluid-stiffness coefficients, no such symmetric property exists. In the past, symmetric and antisymmetric properties have been used based on physical and geometrical considerations [7-9]. These coefficient matrices for a tube row are assumed to be of the form:

Fluid-damping coefficient matrix:

$$\begin{bmatrix} \alpha'_{jk} & \alpha'_{jk} \\ \tau'_{jk} & \beta'_{jk} \end{bmatrix} = \begin{bmatrix} \alpha'_{11} & \alpha'_{12} & \alpha'_{12} & 0 & \sigma'_{12} & -\sigma'_{12} \\ \alpha'_{12} & \alpha'_{11} & 0 & -\sigma'_{12} & 0 & 0 \\ \alpha'_{12} & 0 & \alpha'_{11} & \sigma'_{12} & 0 & 0 \\ 0 & \tau'_{12} & -\tau'_{12} & \beta'_{11} & \beta'_{12} & \beta'_{12} \\ -\tau'_{12} & 0 & 0 & \beta'_{12} & \beta'_{11} & 0 \\ \tau'_{12} & 0 & 0 & \beta'_{12} & 0 & \beta'_{11} \end{bmatrix} \qquad (10)$$

Fluid-stiffness coefficient matrix:

$$\begin{bmatrix} \alpha''_{jk} & \alpha'_{jk} \\ \tau'_{jk} & \beta''_{jk} \end{bmatrix} = \left[\begin{array}{ccc|ccc} \alpha''_{11} & \alpha''_{12} & \alpha''_{12} & 0 & \sigma''_{12} & -\sigma''_{12} \\ \alpha'_{12} & \alpha'_{11} & 0 & -\sigma'_{12} & 0 & 0 \\ \alpha'_{12} & 0 & \alpha'_{11} & \sigma'_{12} & 0 & 0 \\ \hline 0 & \tau'_{12} & -\tau'_{12} & \beta'_{11} & \beta'_{12} & \beta'_{12} \\ -\tau''_{12} & 0 & 0 & \beta''_{12} & \beta''_{11} & 0 \\ \tau''_{12} & 0 & 0 & \beta''_{12} & 0 & \beta''_{11} \end{array}\right] \tag{11}$$

Test results can be used to verify the validity of these assumptions.

Figure 9 shows the fluid-force coefficients α'_{12}, α'_{13}, α''_{12}, α''_{13}, τ'_{12}, τ'_{13}, τ''_{12}, and τ''_{13}. In general, Fig. 9 shows that

$$\begin{aligned} \alpha'_{12} &= \alpha'_{13} , \\ \alpha''_{12} &= \alpha''_{13} , \\ \tau'_{12} &= -\tau'_{13} , \\ \tau''_{12} &= -\tau''_{13} . \end{aligned} \tag{12}$$

These agree with Eqs. 10 and 11. Similar results are found for β'_{12}, β'_{13}, β''_{12}, β''_{13}, σ'_{12}, σ'_{13}, σ''_{12}, and σ''_{13}.

Although the symmetry and antisymmetry properties are valid in general, in some specific reduced flow velocity ranges, Eqs. 12 are not valid. This is probably due to the variation of mean flow across the tube row.

Effects of Oscillation Amplitude and Tube Alignment

Fluid force coefficients are obtained for different oscillation amplitudes, A/D, where A is the peak amplitude. Typical examples are given in Fig. 10. For A/D varying from 0.018 to 0.051, there is no noticeable difference. The maximum magnitude, 0.051, is about 15% of the gap between tubes. This agrees with Tanaka's data [18].

Although fluid force coefficients are not affected by the oscillation amplitude for A/D up to 0.15, large oscillation amplitudes are expected to have a significant influence. As demonstrated in a stability study [19], there are two instability limits, called intrinsic and excited instability. The difference of these two instability limits is partially due to the dependence of fluid-force coefficients on oscillation amplitude.

Figure 11 shows the fluid-force coefficients α'_{12} and α'_{13}, τ'_{12} and τ'_{13} for two cases: (1) tubes 1, 2, and 3 with uniform pitch (solid points on Fig. 11) and (2) tube 2 offset about 0.1 D toward tube 1 (open points on Fig. 11). The results given in Fig. 11 show that the tube alignment causes some variation in fluid-force coefficients.

Fluid-force coefficients depend on tube arrangement and tube alignment. It is expected that misalignment may change fluid-force coefficients; the effect will depend on tube arrangement as well as the amount of deviation.

VI. DISCUSSION

Fluid-damping and fluid-stiffness coefficients of a tube row with a pitch-to-diameter of 1.35 are presented as a function of reduced flow velocity. In addition, the effects of oscillation amplitude, tube alignment and flow velocity are studied. The results agree reasonably well with published data.

The general characteristics of the fluid-force coefficients are noted from the experimental data. These characteristics are important in the study of fluidelastic instability. One of the most important features is that these force coefficients are nominally independent of reduced flow velocity for $U_r > 20$. In this case, fluid-force coefficients can be measured at one value of U_r only, and the force coefficients determined at this U_r will be applicable for all $U_r > 20$. In general, in gas flow, fluidelastic instability occurs at high U_r; therefore it is not necessary to measure fluid-force coefficients as a function of U_r. In addition, two important conclusions can be drawn from the characteristic of constant values of fluid-force coefficients.

- The reduced critical flow velocity is proportional to the half-power of the mass-damping parameter; i.e.,

$$\frac{U}{fD} \alpha \left(\frac{2\pi\zeta m}{\rho D^2}\right)^{0.5} . \tag{13}$$

The proof is given in Ref. 9. Equation 13 is valid regardless of the instability mechanisms and is applicable to both fluid-damping and fluid-stiffness controlled instability.

- The general practice of computing an equivalent uniform velocity as

$$U_e = \frac{\int_o^{\ell} U^2(z)\phi_n^2 dz}{\int_o^{\ell} \phi_n^2(z) dz} , \tag{14}$$

is applicable for large U_r, where U(z) is the axial distribution of crossflow velocity, $\phi_n(z)$ is the mode of interest, ℓ is the tube length, and z is the axial distance parameter. Equation 14 was proposed by several investigators [20-22]. As long as the fluid-force coefficients are independent of U_r, Eq. 14 is valid.

At small values of U_r, both fluid-damping and fluid-stiffness coefficients are functions of U_r. Measurements must be made for the whole range of U_r to establish the values of these coefficients. In this case, Eqs. 13 and 14 are not necessarily valid. More specifically, the following statements can be made:

- At low values of U_r, the critical reduced flow velocity is not necessarily proportional to the half power of the mass-damping values. Furthermore, mass ratio and damping ratio may not be combined as a single parameter.

- The equivalent flow velocity defined by Eq. 14 is not necessarily valid for small U_r.

The symmetric and antisymmetric properties shown in Eqs. 12 are attributed to the specific tube arrangement. In general, fluid-damping and fluid-stiffness coefficients do not possess symmetric characteristics. This is different from fluid-inertia coefficient based on the potential flow.

Fluid-force coefficients depend on tube arrangement and tube pitch. For a given tube array, small tube misalignment apparently is not very important. In addition, fluid-force coefficients are not affected significantly by small-amplitude oscillations.

Fluid-force coefficients based on the unsteady flow theory can be measured experimentally. As demonstrated in this study, measurements of these forces are very tedious. However, at this time, such measurement is the only technique available to obtain these coefficients based on the unsteady flow theory. Analytical methods are not available and numerical techniques are yet to be developed. It is expected that calculations of motion-dependent fluid force will be the subject of future studies in the area of computational fluid dynamics.

ACKNOWLEDGMENTS

This work was performed under the sponsorship of NASA-Lewis Research Center. The authors gratefully acknowledge the support and interest of Drs. Lou Povinelli and John Schwab.

REFERENCES

1. Bishop, R. E., and Hassan, A. Y., "The Lift and Drag Forces on a Circular Cylinder Oscillating in a Flowing Fluid," Proc. Roy. Soc. A. 277, 51-75 (1964).

2. Toebes, G. H., and Ramamurthy, A. S., "Fluidelastic Forces on Circular Cylinders," J. of the Eng. Mechanics Div., Proc. ASCE, EM6, 1-21 (1967).

3. Protos, A., Goldschmidt, V. W., and Toebes, G. H., "Hydroelastic Forces on Bluff Cylinders," Trans. ASME, J. of Basic Eng. 90, 378-386 (1968).

4. Tanaka, H., and Takahara, S., "Study on Unsteady Aerodynamic Forces Acting on an Oscillating Cylinder," Proc. of the 19th Japan National Congress for Applied Mechanics, Paper No. IV-9, pp. 162-166 (1969).

5. Staubli, T., "Calculation of the Vibration of an Elastically Mounted Cylinder Using Experimental Data from Forced Oscillation," ASME, J. of Fluids Eng. 105, 225-229, (1983).

6. Tanida, Y., Okajima, A., and Watanabe, Y., "Stability of a Circular Cylinder Oscillating in a Uniform Flow or in a Wake," J. Fluid Mech. 61, 769-784 (1973).

7. Tanaka, H., and Takahara, S., "Fluidelastic Vibration of Tube Array in Cross Flow," J. Sound Vib. 77(1), 19-37 (1981).

8. Tanaka, H., Takahara, S., and Ohta, K., "Flow-Induced Vibration of Tube Arrays with Various Pitch-to-Diameter Ratio," J. Pressure Vessel Technol. 104, 168-176 (1982).

9. Chen, S. S., and Jendrzejczyk, J. A., "Stability of Tube Arrays in Crossflow," Nucl. Eng. Des. 75(3), 351-373 (1983).

10. Chen, S. S., "A General Theory for Dynamic Instability of Tube Arrays in Crossflow," To appear in J. Fluids and Structures.

11. Chen, S. S., "Vibration of Nuclear Fuel Bundles," Nucl. Eng. Des. 35, 399-422 (1975).

12. Chen, Y. N., "Flow-Induced Vibration and Noise in Tube Bank Heat Exchangers due to von Karman Streets," ASME J. Eng. for Industry 90, 134-146 (1968).

13. Borges, A. R. J., "Vortex Shedding Frequencies of the Flow Through Two-Row Banks of Tubes," J. Mech. Eng. Sci. 11(5), 498-502 (1969).

14. Clasen, P., and Gregorig, R., "Ein Schwingungskriterium eines querangeströmten Rohres," Chemie Ing. Tech. 43, 982-985 (1971).

15. Ishigai, S., Nishikawa, E., and Yagi, E., "Structures of Gas Flow and Vibration in Tube Banks with Tube Axes Normal to Flow," Int. Symp. on Marine Eng., Tokyo, pp. 1-5-23 to 1-5-33 (1973).

16. Auger, J. L., and Coutanceau, J., "On the Complex Structure of the Downstream Flow of Cylindrical Tube Rows at Various Spacings," Mech. Res. Comm. 5(5), 297-302 (1978).

17. Chen, S. S., "Instability Mechanisms and Stability Criteria of a Group of Circular Cylinders Subjected to Crossflow; Part 2: Numerical Results and Discussions," J. Vibration, Acoustics, Stress, and Reliability in Design 105, 253-260 (1983).

18. Tanaka, H., "Study on Fluidelastic Vibration of Tube Bundle," ANL-Trans-1191, Translated from Japanese in Transactions of the JSME, Section B, 46, 1398-1407 (1980).

19. Chen, S. S., and Jendrzejczyk, J. A., "Instability Characteristics of Fluidelastic Instability of Tube Rows in Crossflow," Argonne National Laboratory Report ANL-86-21 (1986).

20. Connors, H. J., "Fluidelastic Vibration of Heat Exchanger Tube Arrays," J. Mech. Des., Trans. ASME 100, 347-353 (1978).

21. Pettigrew, M. J., Sylvestre, Y., and Campagna, A. O., "Vibration Analysis of Heat Exchanger and Steam Generator Designs," Nucl. Eng. Des. 48, 97-115 (1978).

22. Franklin, R. E., and Soper, B. M. H., "An Investigation of Fluidelastic Instabilities in Tube Banks Subjected to Fluid Cross-Flow," 4th SMiRT, Paper No. F6/7 (1977).

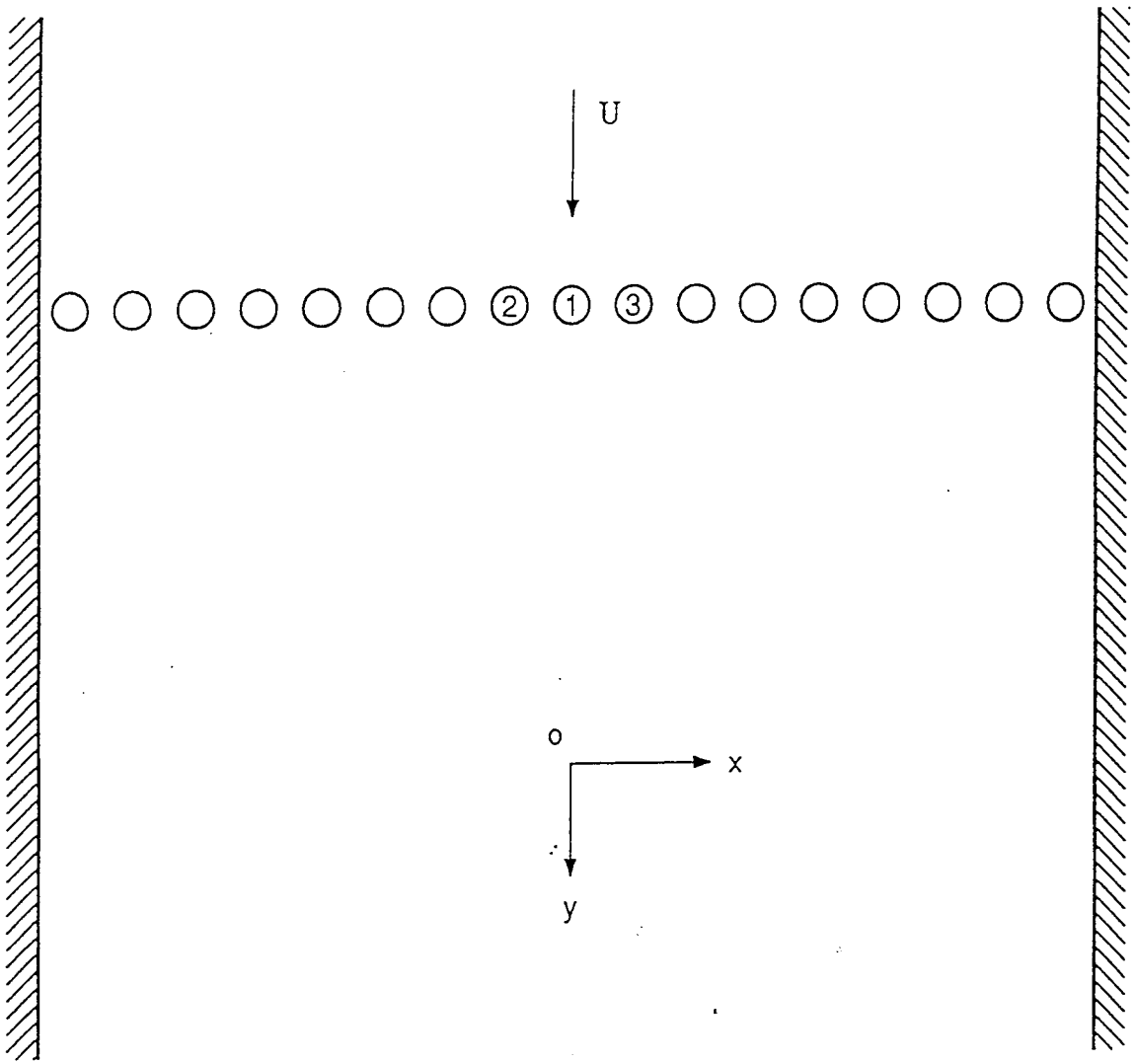

Fig. 1. Row of tubes in Crossflow

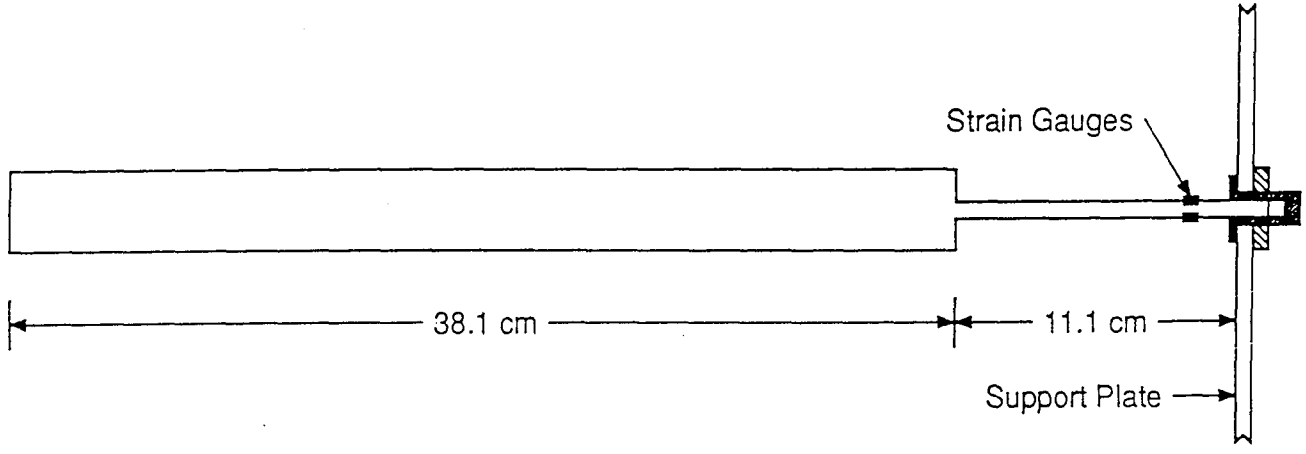

Fig. 2. Schematic of an Active Tube

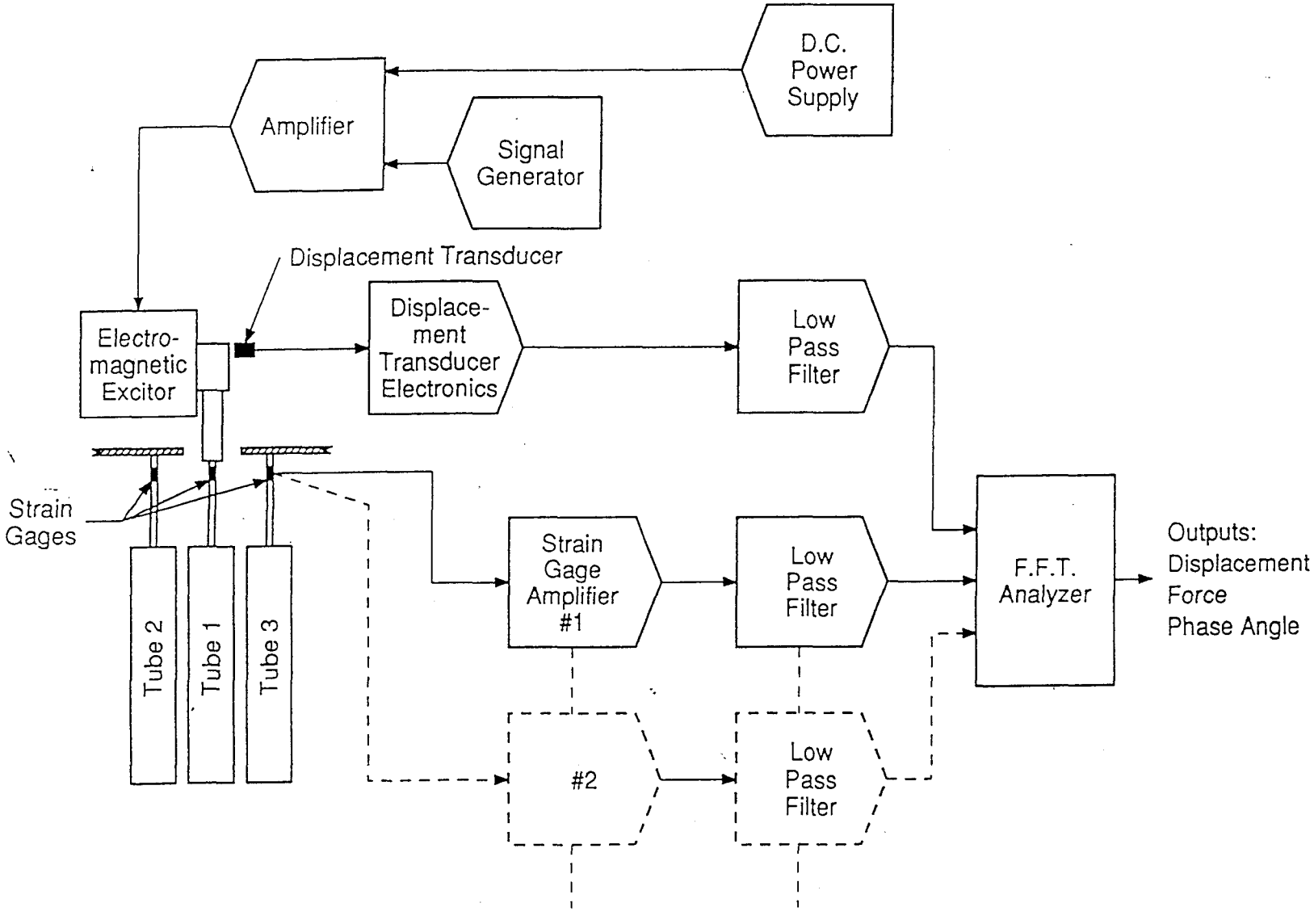

Fig. 3. Data Analysis

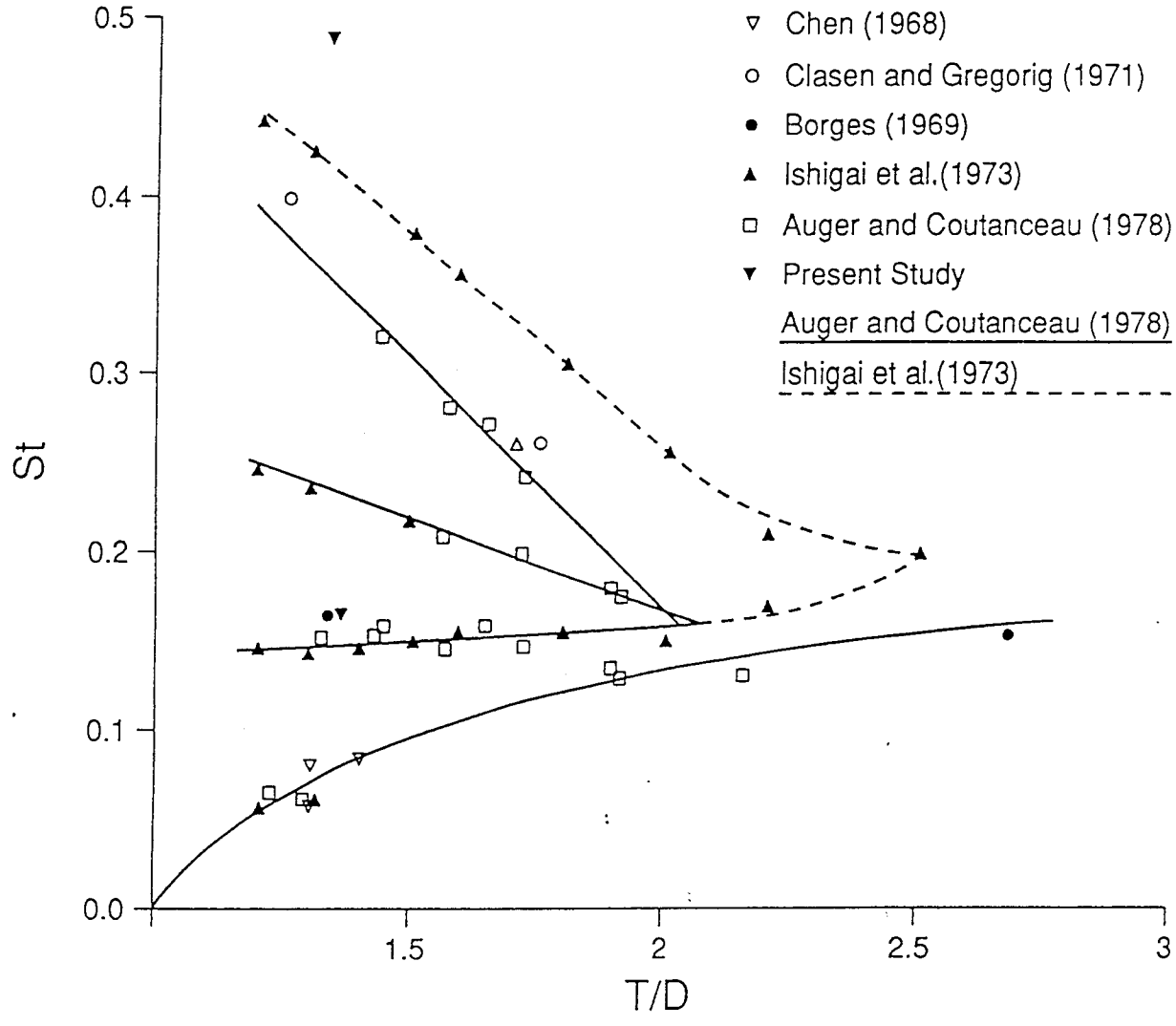

Fig. 4. Strouhal Number for Tube Row as a Function of Pitch-to-Diameter Ratio

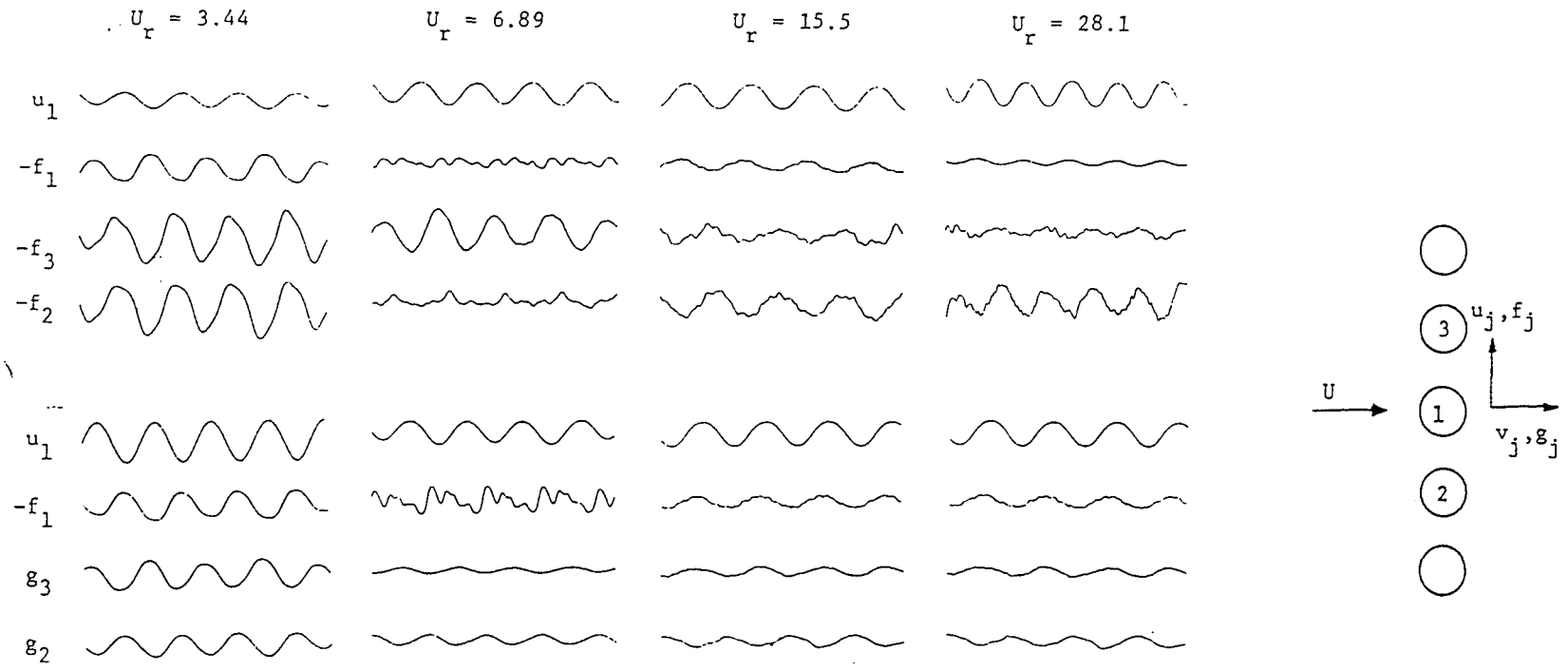

Fig. 5. Fluid Force Components Acting on a Tube Row

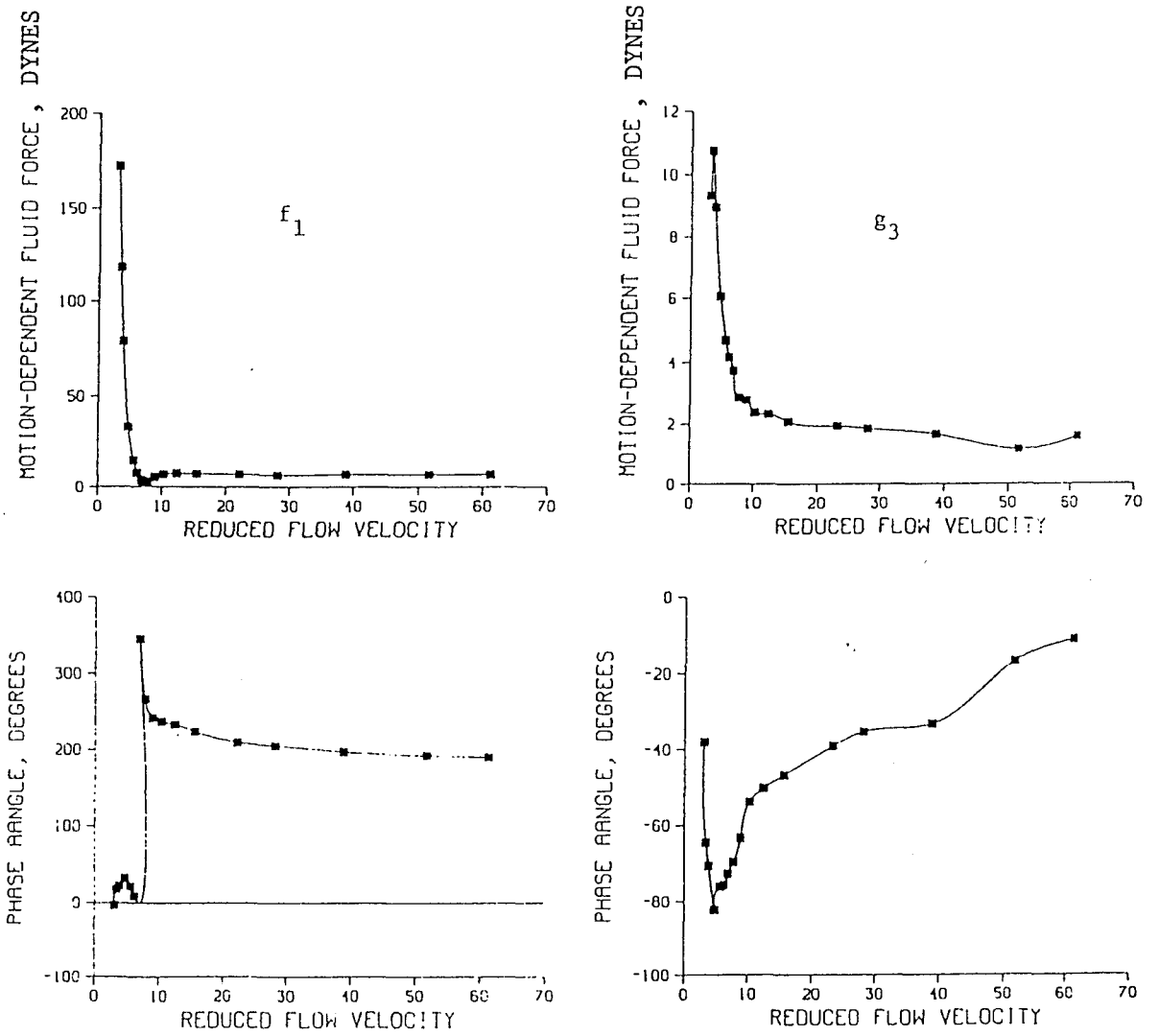

Fig. 6. Magnitude of Fluid Force and Phase Angle between Fluid Force and Tube Displacement

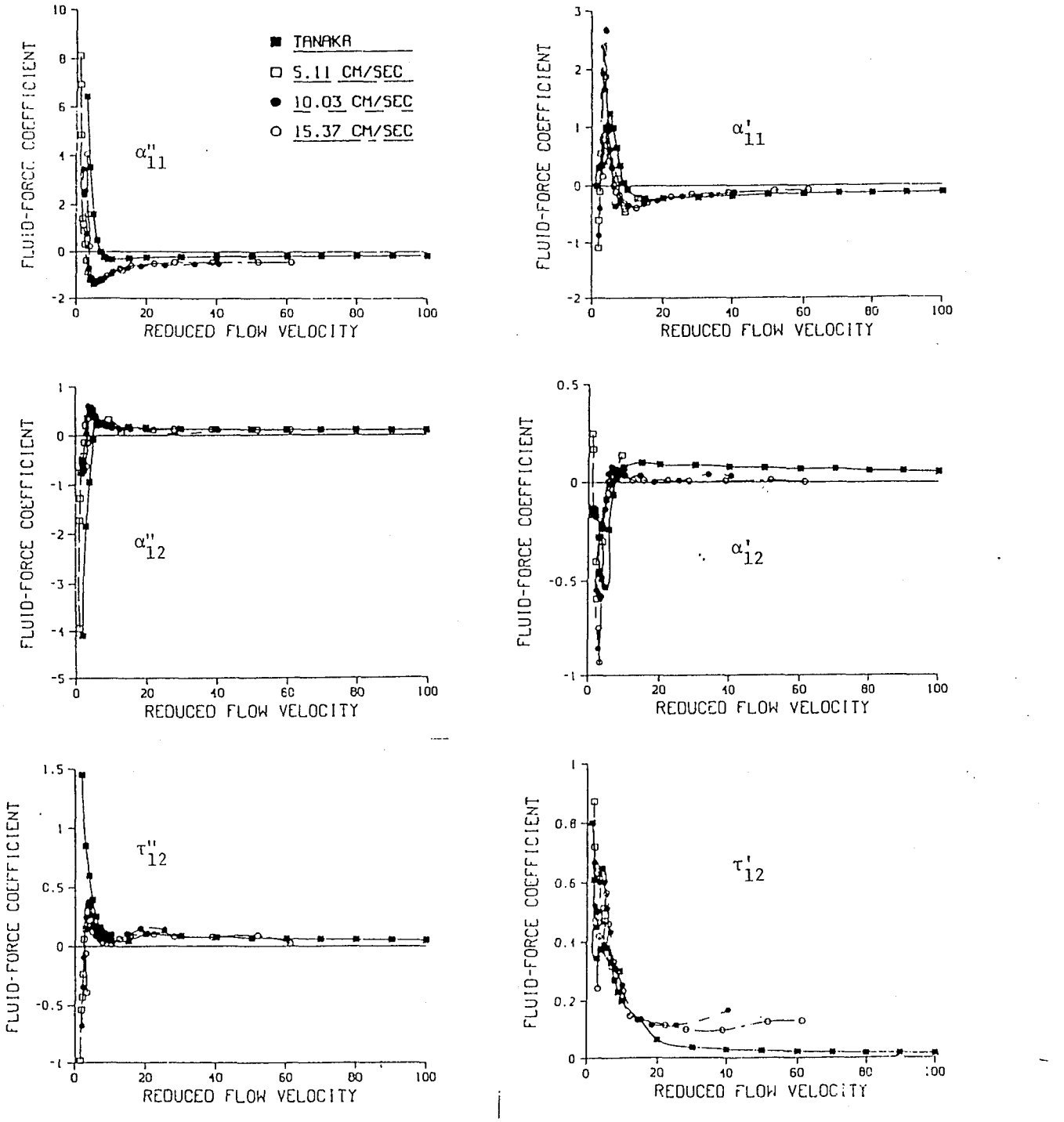

Fig. 7. Fluid-Force Coefficients α'_{11}, α''_{11}, α'_{12}, α''_{12}, τ'_{12}, and τ''_{12}

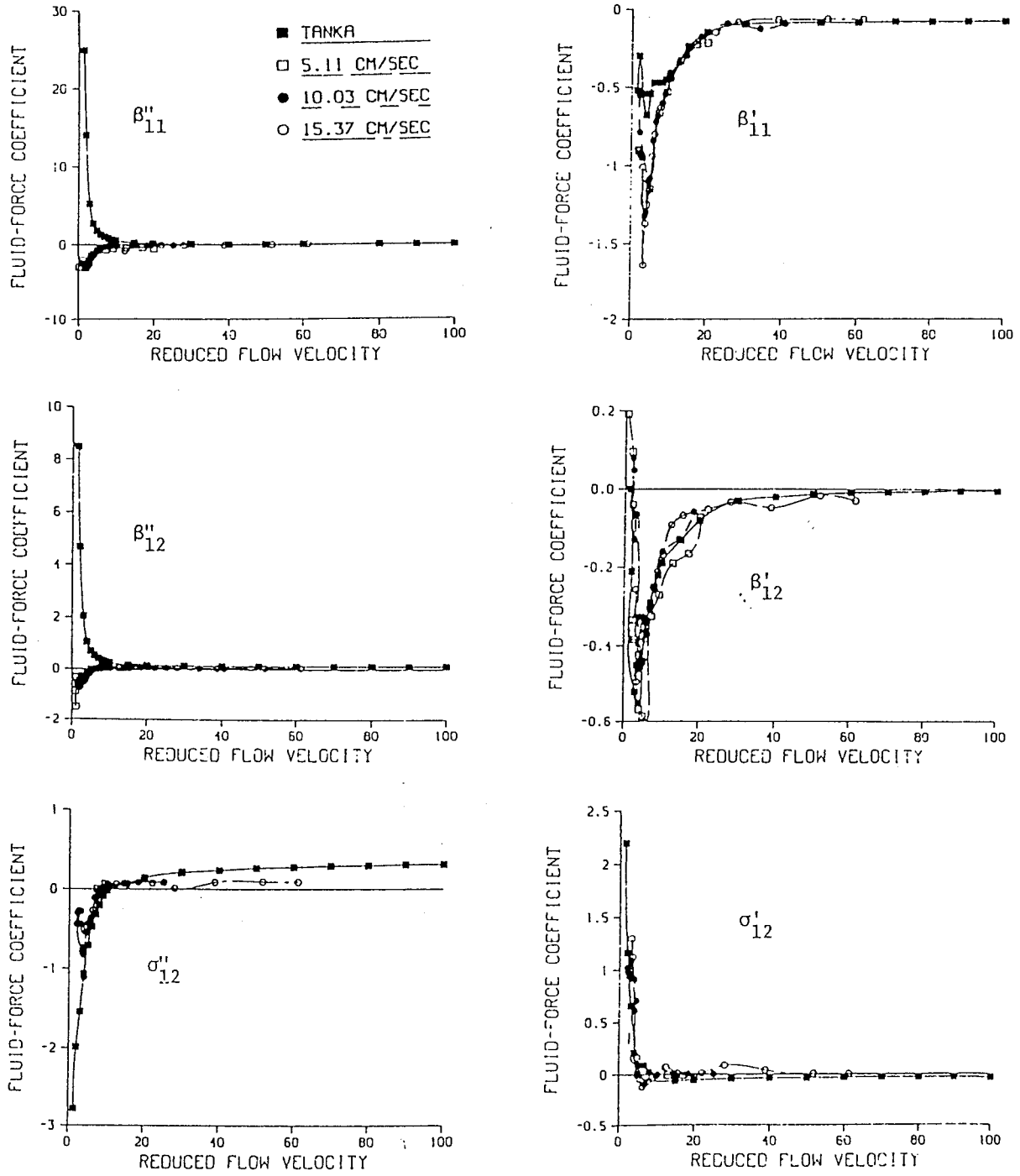

Fig. 8. Fluid-Force Coefficients β'_{11}, β''_{11}, β'_{12}, β''_{12}, σ'_{12}, and σ''_{12}

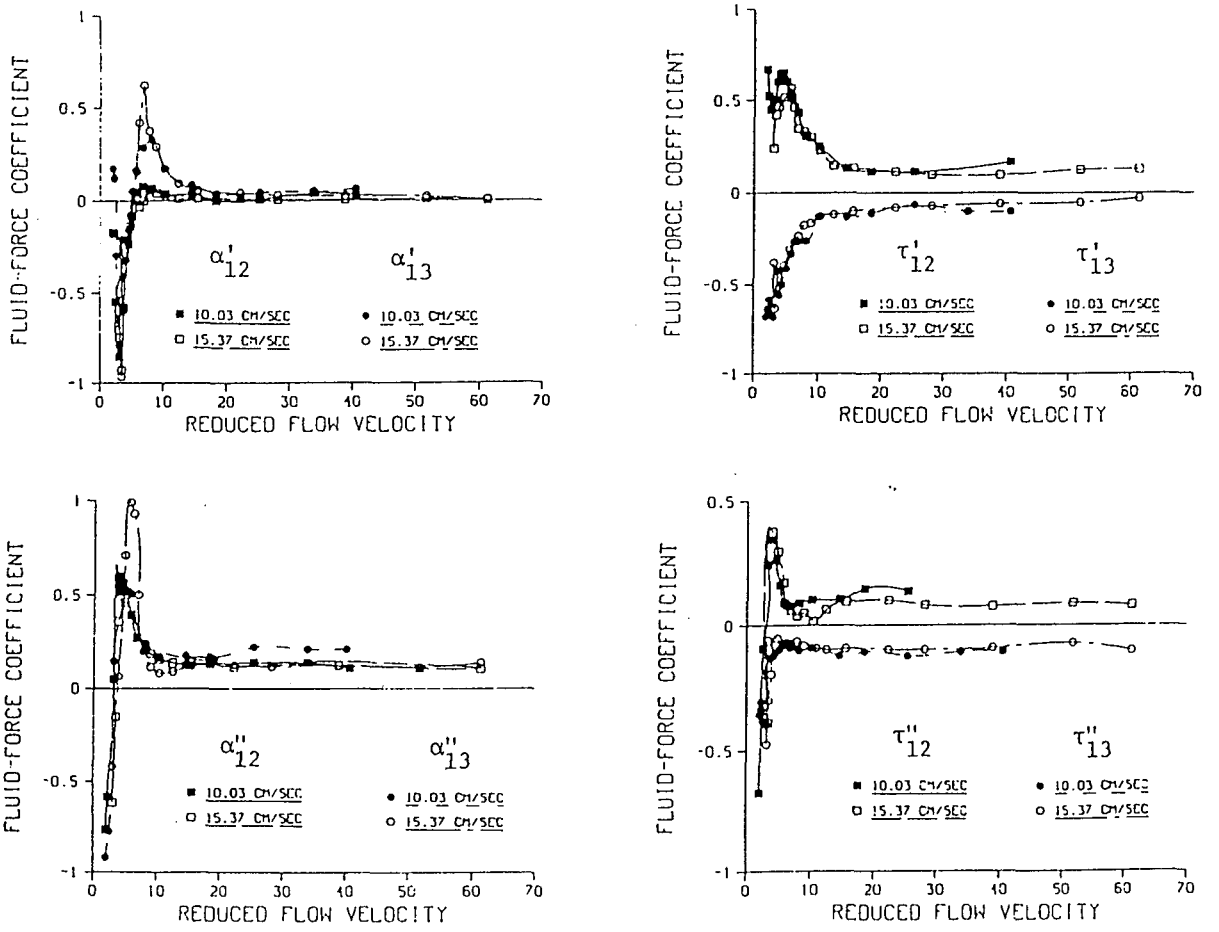

Fig. 9. Symmetry and Antisymmetry of Fluid-Force Coefficients

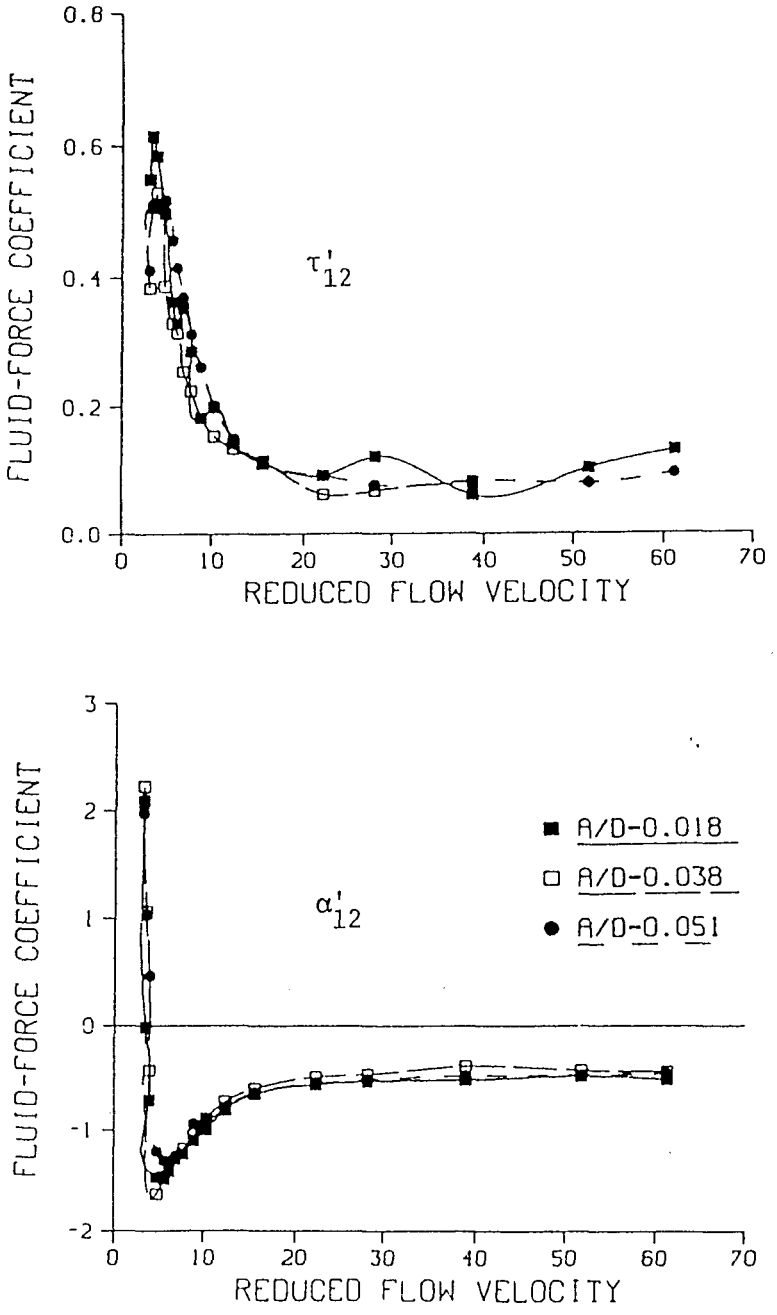

Fig. 10. Effect of Tube Alignment on Fluid-Force Coefficients

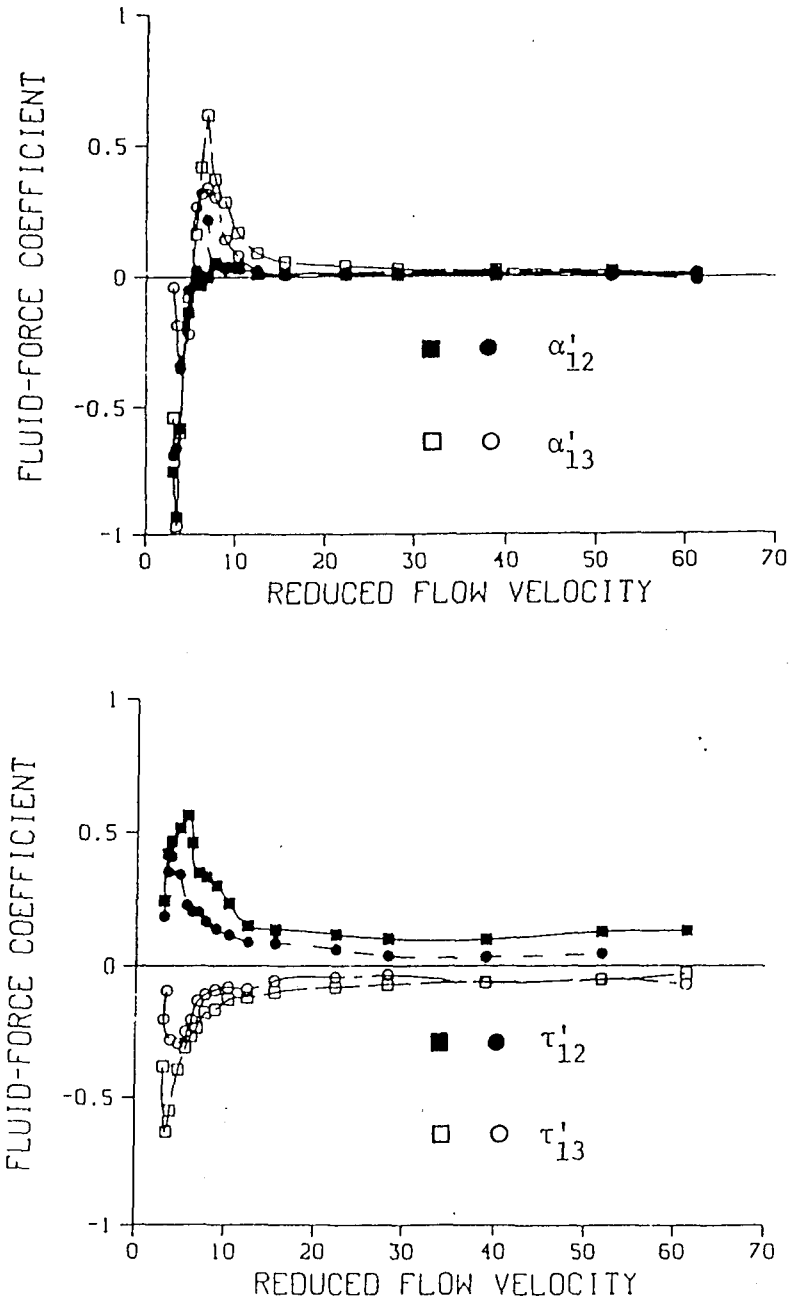

Fig. 11. Effect of Oscillation Amplitude on Fluid-Force Coefficients